Probing Internal Stress and Crystallinity in Wet Foam *via* Raman Spectroscopy

T. K. Barik, P. Bandyopadhyay and A. Roy*

Department of Physics, Indian Institute of Technology Kharagpur 721 302, India

Abstract

In this article, we correlate the internal stress and the characteristics of a vibrational mode in wet foam. Using microscope images, we estimate the average size of the bubbles in wet foam, at specific time intervals, over a duration of twenty four hours. Raman spectra are also recorded at the same time intervals, over the same time frame. We show that the internal stress, originated from the macroscopic structural change of foam with ageing, can be related to the observed Raman shift of the low frequency methylene rocking mode of the constituent surfactant molecules in foam. In this report we also show the capability of the Raman spectroscopy to reveal the crystallinity in foamy materials, when studied for a longer period of time.

*Electronic address: anushree@phy.iitkgp.ernet.in

I. INTRODUCTION

Soft foam, a cellular fluid, is a two phase system. It consists of a collection of gas bubbles surrounded by thin liquid films. With time, the spherical bubbles in fresh foam take the form of polyhedra while minimizing the energy of the system. It can coarsen by the diffusion of gas from smaller bubbles to larger bubbles [1]. Furthermore, the liquid between the bubbles can drain out along the liquid channels (Plateau borders) in response to gravity. The adjacent bubbles coalesce if the liquid film becomes too thin.

Soft foam exhibits interesting elastic properties. Under low applied shear stress, foam behaves as an elastic solid. With an increase in stress it becomes progressively plastic; beyond a certain yield stress, the foam flows along with topological changes. Such characteristics of foamy structure strongly depends on bubble size and wetness [2]. Both two- and three dimensional foam can be accurately simulated using various models [3]. The computer simulation results suggest that, in the low compression limit, there exists a correlation between the shear modulus and gas/liquid fraction in the tightly packed gas bubbles [4, 5, 6, 7, 8, 9]. These models, therefore, reveal a connection between the complex macroscopic rheological behavior of foam and its underlying microscopic structure.

The complex foam structure is composed of extended polyatomic organic molecules (surfactants) and water. Raman spectroscopy is a powerful noninvasive tool to probe the molecular structure and dynamics of a system. In wet foam, Raman scattering is caused by deformation/stretching of different vibrational bonds of constituent molecules. Thus, if it is assumed that macroscopic and microscopic behavior of wet foam can be related, one expects that the analysis of Raman line profiles, which reveal molecular behavior, can be used to probe the elastic properties of wet foam. The stress induced shift in the Raman lines has

been reported for other soft matter, like soft polymers and polymer based fiber structures [10, 11]. For example, it has been shown by Ward and Young, via polarized NIR Raman measurements, that Raman bands of thermotropic aromatic copolyesters exhibit linear shifts towards lower wavenumbers with stress and strain following the tensile deformation [12]. The correlation between the architecture of the network and elastic properties of their building blocks leads to interesting mechanical properties of such systems [13]. The main difficulty in using Raman spectroscopy to probe wet foam arises due to multiple scattering of light within the bubbles. The broad and strong background due to the scattered light masks the Raman signal from the foamy structure by a large extent. Thus, in the literature, we do not find too many articles on Raman studies of wet foam. The most significant one is by Goutev and Nickolov [14], where the authors have studied the molecular structure of Gillette foam, to some extent, using Raman spectroscopy. Recently, we have reported our results on Raman measurements in Gillette foam, where we have analyzed the evolution of the O-H vibrational bond of water molecules with ageing [15].

In this article, we probe, using Raman scattering, how the macroscopic changes in structure of bubbles in wet foam is manifested in changes in the molecular structure of the surfactant molecules. Section II explains the reasons for the choice of our sample and also describes other experimental details. The structural changes in foam with time have been described in Section III. In Section IV, we have shown the effect of structural change in wet foam on the molecular vibrational modes of Gillette foam, as obtained from Raman measurements. We correlate the change in molecular vibrations with the evolution of internal stress and crystalline structure of foam. Finally, in Section V, we summarize our results with a few remarks.

II. EXPERIMENT

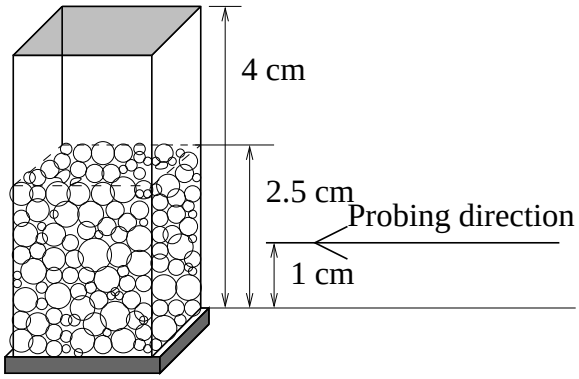

FIG. 1: The schematic of the foam container and the probing direction.

Though complex in composition, Gillette shaving foam is often used for studying optical properties of wet foam. It is reproducible and stable over the duration required for optical measurements. For Raman measurements this commercial foam offers an extra advantage in the following sense. When laser light is incident on foam, it undergoes multiple scattering. In order to obtain the optimum Raman signal, the mean free path, $l^{\star}$,[$\cong$ 3.5 $\times$ average diameter of the bubbles (d)] of light within the foam should be comparable with the slit width of the spectrometer collecting the scattered light [14]. The mean diameter of bubbles in fresh Gillette shaving foam is close to 50 μm and the maximum diameter, which we have studied, is $\sim$ 150 μm, which is comparable with the slit-width of our spectrometer ($\sim$ 100 μm).

In this commercial foam, the basic ingredients [triethanolamine stearate with small amount ($< 1\%$) of sodium lauryl sulphate and polyethylene glycol lauryl ether and emulsified liquid hydrocarbon gases] are kept in an aqueous solution under high pressure. The foam is produced after expansion of the above mixture in the aqueous solution. The experiments have been carried out by taking the foam from the can in a closed rectangular quartz cell of

dimension 1cm × 1cm × 4cm [Fig. 1]. In the beginning, the material fills ∼ 2.5 cm of the whole cell volume from the bottom. The cell is then sealed with paraffin films to prevent direct evaporation. Raman measurements and imaging experiments have been carried out at a distance 1 cm from the bottom of the cell [Point P in Fig. 1]. To observe the effect of ageing, the measurements have been continued at the same point throughout the duration of the experiment. The experiments have been repeated for two other heights on the column of foam to check the reproducibility of the results.

The change in the structure of foam with aging, is probed through optical images using a Metzer Biomedical microscope (model: MEGA-6021). These images are analyzed using Image-J image-processing software. Simultaneously, Raman spectra are recorded in a back-scattering geometry using TRIAX550 single monochromator equipped with a notch filter and CCD as a detector. An argon ion laser of wavelength 488 nm and of power 30 mW on the sample has been used as an excitation source. For more details of the technique and spectrometer, see [16]. As the spot size of the laser, used as an excitation source in Raman measurements, is ∼ 0.5 mm (much more than the size of the channels between bubbles or Plateau border region); at present, it is not possible for us to distinguish, whether the measured Raman signals are confined only to the Plateau border region or within the thin film between two bubbles or in both. All measurements and analysis of data have been carried out for three different sets of experiments to check the reproducibility of the results. Raman spectra are fitted with Lorentzian line shape keeping peak position, width and intensity as fitting parameters in order to estimate them properly, for each observed feature.

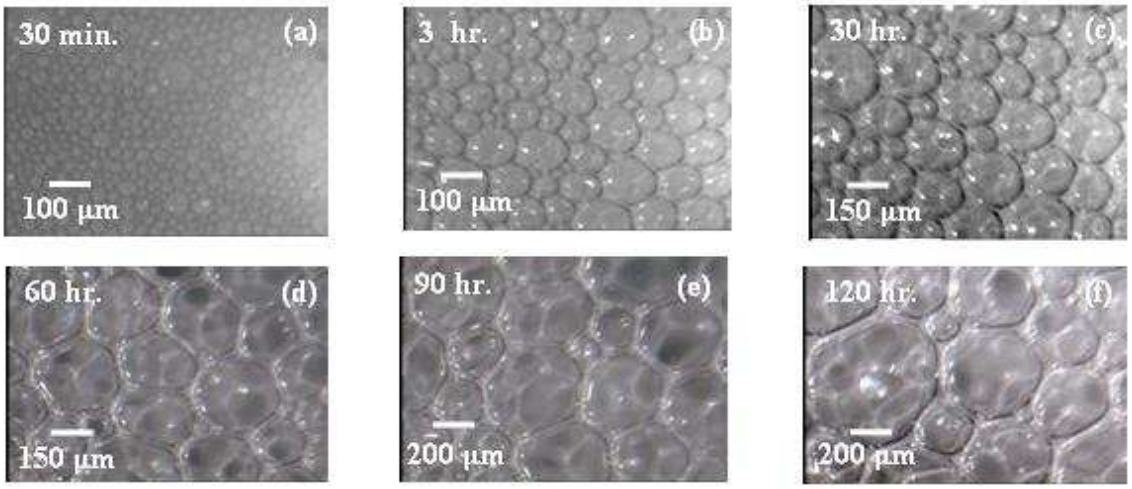

FIG. 2: Microscopic images of liquid foam at different time scale: the corresponding magnification of the images are shown in each figure.

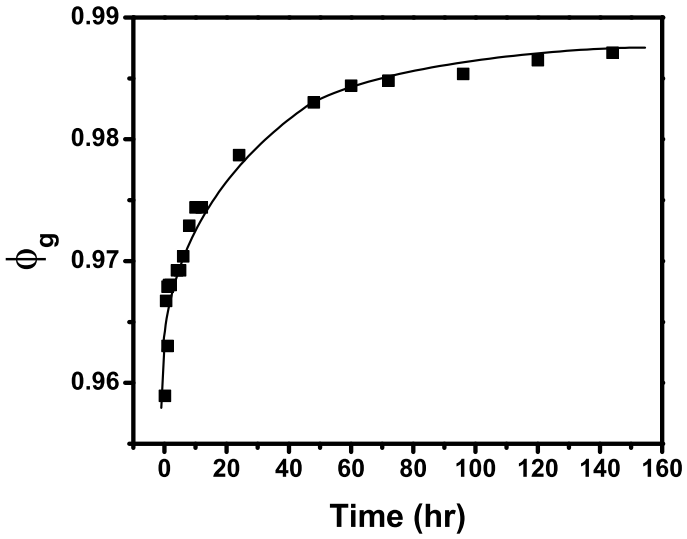

FIG. 3: Variation in gas fraction with aging. The solid line is a guide to the eye.

III. SHAPE AND STRUCTURE

As mentioned earlier, aging effects on foam structure can be seen through microscopy. More precisely, we recorded the images of foam at an interval of 15 minutes in the beginning (till 12 hrs) and less frequently at the end, over 7 days. Fig.2(a) to (f) show few characteristic

microscopic images at different stages of aging. Initially, the bubbles are spherical, separated by Plateau borders touching the quartz cell wall. Subsequent snapshots show that the bubbles take on a polyhedral structure due to coarsening of the bubbles and liquid drainage.

The three-dimensional (3D) gas fraction, (ϕ_g), is the commonly used parameter to describe a foam. ϕ_g can be estimated from the following relation

$$\phi_g = 1 - \frac{\rho_1}{\rho_2}, \tag{1}$$

Here, ρ_1 and ρ_2 are the mass densities of the foam and the liquid phase (ρ_2=0.997 gm/cc [17]). Foam mass density was obtained from the measured weight of the foam. The variation in 3D-gas fraction with time is shown by filled square in Fig. 3(b). The solid line is the guide to the eye. It is to be noted that the gas fraction varies for the foam expelled from different portions of the can [14].

IV. MOLECULAR VIBRATIONAL BANDS - RESULTS AND DISCUSSION

A. Low frequency methylene rocking mode

In the Raman spectrum of Gillette foam, the time evolution of the out of plane methylene rocking modes, at around 725 cm^{-1} [18], is shown in Fig. 4. The intensity is scaled to show the variation in spectral frequency with the ageing of foam. Here, we have shown a few characteristic spectra; though we recorded the Raman spectrum over the same period and at similar intervals, as was done in the imaging experiment. This Raman line corresponds to the trans- conformation of the methylene chain. The direction of the arrow is along the increase in time (the average diameter of the bubbles increases during the ageing process). Interestingly, the Raman shift of the peak at around 725 cm^{-1} exhibits a non-monotonous behavior with ageing (see the dotted red line).

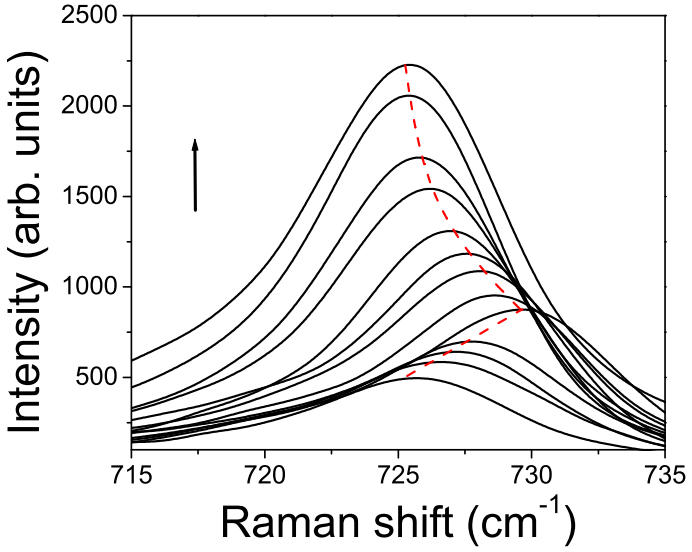

FIG. 4: The variation in the methylene rocking modes due to aging of Gillette foam. The direction of the arrow is along the increase in average diameter of bubbles (43,75,93,117,135,144,157,182,222, 283,318, 400 and 440 μm). The red dashed curve is a guide to the eye to show the non-monotonic variation in Raman shift.

At this point we draw an analogy between the behavior of a solid and a foam network. For solids, the magnitude of the shift in Raman wavenumber for the modes of quantized lattice vibration can be related to the component of the stress tensor of the system along different directions via a constant, which has the unit of frequency change per unit stress [19]. A compressive stress results in a higher wavenumber shift in the Raman line, whereas, a tensile stress shifts the Raman line in the opposite direction. To the best of our knowledge, any such study on a foamy structure is not available in the literature. Nevertheless, it is to be noted that soft matter exhibits behavior, which is, at times, closer to that of a solid. The surfactant molecules are fastened together in a group rather rigidly and are constrained at the mesoscopic scale to behave more like a solid. The interaction of the constituent molecules within these groups determine the macroscopic behavior of foam. On the other hand, these

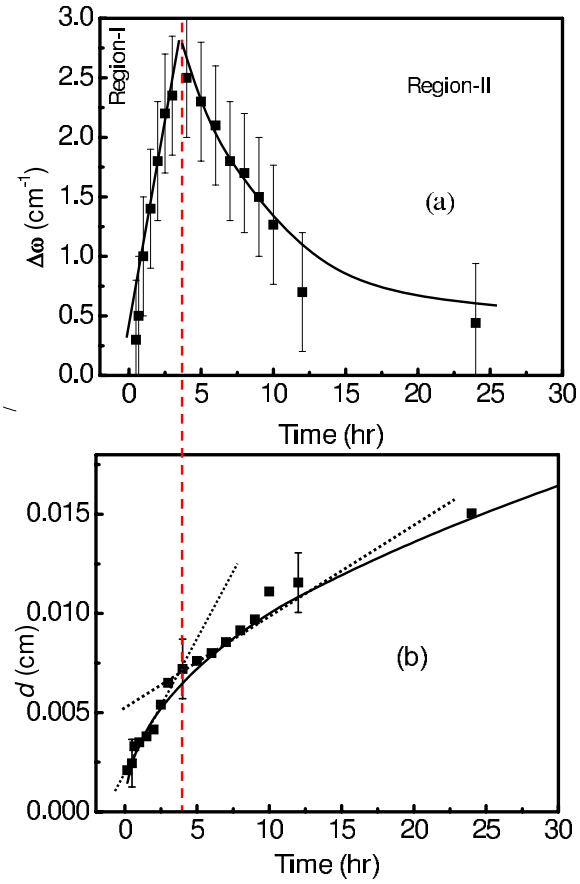

FIG. 5: (a) A plot of $\Delta\omega$ vs t for methylene rocking mode as observed from Raman measurements (filled squares) as obtained from Fig. 4. The solid line is a guide to the eye. (b)Variation in average bubble diameter with aging.

molecular groups do move like the molecules in a simple fluid [20]. In view of these facts, we attempt to explain the non-monotonous change in Raman shift, as shown in Fig. 4, by assuming a correlation between the Raman shift of the vibrational mode and the internal stress in wet foam, as done in the case of solids.

We define the difference between the Raman frequency (ω_t) of the above mode from the surfactant of foam at time t, and the Raman frequency of the same (ω_0) in fresh Gillette foam as $\Delta\omega$ ($\Delta\omega = \omega_t - \omega_0$). The variation of $|\Delta\omega|$ with t, is shown in Fig. 5(a) [filled squares]. The magnitude of the difference ($\Delta\omega$) increases with increase in t till $t = t' \sim 4$

hr (Region I, the left hand side of the dashed-red line, in Fig. 5), indicating a compressive stress in the liquid film to be the origin of the shift. Then it decreases with a further increase in time (Region II, the right hand side of the dashed-red line, in Fig. 5), indicating a gradual release of the stress.

To explain the above variation of stress with time in wet foam, we take a re-look at the variation in average bubble diameter d with time (a few characteristic image frames are shown in Fig. 2). Assuming the bubbles to be nearly spherical at all stages, we measured the average diameter of 200 bubbles for each time frame. In Fig. 5(b) the variation in measured d with time is shown by the filled squares. The time scale of evolution of the cellular pattern can be taken to be inversely proportional to the length scale. Hence, the average diameter of the bubbles follows the scaling behavior [21, 22],

$$d \propto (t - t')^{1/2}. \tag{2}$$

Here, t' is a constant. In Fig. 5(b) the best fitted line to the data points with Eqn. 2, is shown by the solid line. In a strict sense, Eqn. 2 is valid for dry foam [23]. This explains the slight deviation of the fitted line from the experimental data in Fig. 5(b). Here it is interesting to note that the smooth variation of d with t in Fig. 5 (b) can be decomposed into two parts with two distinct slopes (shown by dotted black lines). Again we find that in Region I, ie. till time t= 4 hr. (same time during which the compressive stress on the molecules reaches maximum in Fig. 5(a)) the increase in d with t is relatively sharp, then it gradually slows down.

When the diameter of a bubble in fresh foam fluctuates to one which is infinitesimally larger in size, the diameter of the neighboring bubble shrinks by the same amount. Due to the larger internal pressure in the smaller bubble, the air flows from it to the larger bubble. As a result, the size of the smaller bubble decreases further in size. This phenomenon causes

an increase in average bubble diameter in foam. The relatively rapid increase in diameter of the bubble in Region I in Fig. 5 (b) compresses the liquid film between bubbles, resulting in a compressive stress in the film (a 'jamming' effect), shown in Region I of Fig. 5 (a). At this point we refer to the pioneering work by Friberg and Langlois [24], where it has been shown that two phases can exist in wet foam. Though the liquid phase in foam is known to be isotropic at the initial stage, with ageing, the formation of lamellar phase results in the crystal-like structure in foam [14]. The small lamellae gets parallel to the interface and gradually forms a large bilayer structure. The interface of gas-liquid has a noticeable effect on this lamellar phase, more than what is observed for the isotropic phase [25]. For a spherical bubble in a liquid, the pressure difference between the gas-liquid interface normally confirms the Laplace-Young law. The Laplace pressure acting outward on the surface is given by $\Delta p = \frac{4\gamma}{R}$, with γ being the surface tension between gas-liquid interface and R being the local radius of curvature of the surface. Due to the formation of lamellar phase in foam at a later time, the pressure acting in the film between bubbles is gradually released with an increase in R. Also note that at a later time (Region II in Fig. 5), the growth rate is also less. In addition, we need to keep in mind that from a wet foam liquid drains out with time. All three effects, effectively, cause a release in pressure in the film. Fig. 5(a) and (b) possibly indicate two coupled and competitive dominating phenomena (coarsening and drainage) in the ageing process of the foam.

In the above, we have tried to explain the variation of the Raman frequency of one of the strongest molecular vibrational modes of Gillette foam by taking into account the internal stress in the system. We would like to mention that, such an effect of aging on Raman shift has not been observed for other vibrational modes in wet foam [14]. A possible explanation can be that the other features corresponding to stretching molecular vibrations, are, usually,

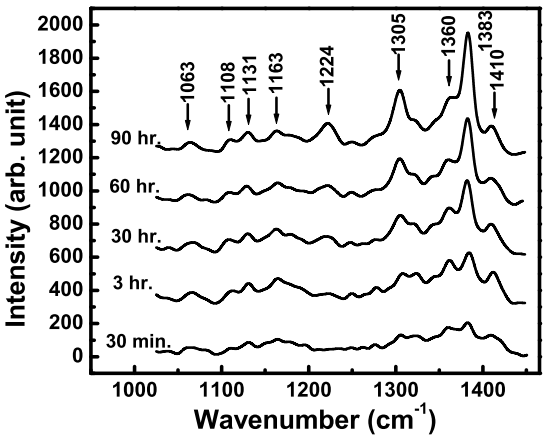

FIG. 6: The change in Raman spectrum of Gillette foam with aging in the region between 1000 and 1450 cm^{-1}.

convoluted with many other modes and therefore, this effect is masked. Moreover, the effect of internal shear (which eventually cancels out when we take ensemble average) in foam is expected to be more for angular deformation of the local bonds rather than bond stretching.

B. Characteristics of other C-H vibrations

To illustrate the time evolution of the molecular structure of Gillette foam, few characteristic Raman spectra over the range between 1000 and 1450 cm^{-1} are shown in Fig. 6. The experiments have been carried out for 7 days. The main features are indicated by arrows. Four types of vibrations are observed, namely stretching and deformation of C-H and C-C bonds. The peaks at 1063 and 1131 cm^{-1} are the in-phase and out-of-phase C-C rocking vibrational modes for the functional group $\diagdown\!\!\diagup C(CH_3)_2$. These features indicate trans intra-molecular conformation. Here we would like to point out that for gauche conformation, the Raman lines are expected to appear between 1085 and 1095 cm^{-1}, which are absent in Fig. 6. In addition, here we mention, especially, the following features. The C-C skeletal

vibration in -$C(CH_3)_3$ functional group and C-H symmetric vibration of the -CH_3, which appear at 1224 cm^{-1} and 1383 cm^{-1}. One expects two overlapping bands, one at 1368 and the other at 1352 cm^{-1}, due to C-H deformation vibrations in CH. These two features merge and appear as one peak at 1360 cm^{-1}. The C-H deformation vibration in -$(CH_2)_n$- appears at around 1305 cm^{-1}, the intensity of this feature in expected to increase with n. All the above features along with others, shown by arrows in Fig. 6, and their assignments are tabulated in Table I.

TABLE I: Assignment of Raman vibrational bands between 1000 to 1450 cm^{-1} for Gillette foam

Assignment	Wavenumber (cm^{-1})	Ref.
C-C rocking mode in $\diagdown\!\diagup C(CH_3)_2$	1063 & 1131	[14]
C-C stretching mode in $\diagdown\!\diagup C(CH_3)_2$	1163	[26]
C-C stretching in phospholipid bilayer	1108	[14]
C-C skeletal vibration in -$C(CH_3)_3$	1224	[26]
C-H deformation vibration in -$(CH_2)_n$	1305	[18]
C-H deformation vibrations in CH	1360	[26]
C-H symmetric vibration in -CH_3	1383	[26]
acyl chain of polyethylene	1410	[27]

From Fig. 6 it is clear that except the intensities of the features at 1383,1305, and 1224 cm^{-1}, the intensities of the other peaks remain nearly constant with aging. The increase in intensities of the Raman lines at 1224 and 1305 cm^{-1} indicate formation of longer polymeric chains, $(CH_3)_3$ and $(CH_2)_n$, with the aging of foam. Vibrational spectra of the C-H stretching region are complex due to Fermi-resonance interactions between the symmetric methylene C-H stretching mode and the overtones of the CH_2 rocking modes. Unlike the C-H stretching vibrations, the CH_2 rocking modes participate significantly in intermolecular coupling and are thus influenced by the lateral packing order. Due to the Fermi resonance interaction of

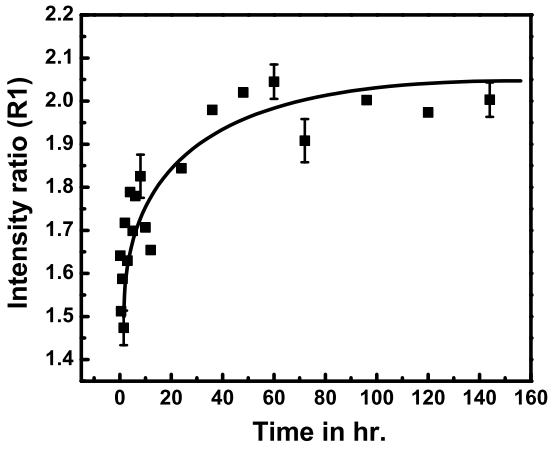

FIG. 7: The variation of intensity ratio (R1) of the Raman lines at 1305 and 1383 cm^{-1} with aging of foam.

CH_2 rocking with symmetric C-H stretching, the latter indirectly gets affected by the lateral packing order. On the other hand, the asymmetric C-H stretching mode is forbidden by symmetry for Fermi-resonance interactions and is thus insensitive to the lateral ordering. Thus, one can expect that the asymmetric vibrational mode at 1305 cm^{-1} should depend only on chain conformation, while the symmetric vibrational mode at 1382 cm^{-1} should be modified by the lateral packing order. Consequently, the ratio (R1) of intensity of the feature at 1305 cm^{-1} to that at 1383 cm^{-1} can be used as a parameter which is sensitive to both the lateral packing and to conformational order within the chains. The variation of the ratio R1 with t is shown in Fig. 7. The value of this ratio is expected to be 0.7 for completely melted hydrocarbon chains, 1.5 for vibrationally decoupled all-trans chains, and 2.2 for a highly ordered crystalline lattice [28]. From Fig. 7 it is clear that the surfactant molecules undergoes a gradual structural change with time. After $\sim$ 40 mins the value of R1 reaches the value $\sim$ 1.6, indicating that the constituent molecules are in trans conformation, however gradually they organize into an ordered multilayer or crystal structure (with R1 =

2.1).

V. SUMMARY

As far as we know, this is the first report where Raman spectroscopy has been used to determine the internal stress in wet foam. In other words, here we have shown that Raman spectroscopy has the potential to extract information about internal stress in the system. We have related the observed shift in the low frequency Raman peak position of the methylene rocking mode with the variation in internal stress in the system.

The composition of commercial shaving foams is quite complex and its physico-chemical properties are ill defined. Though, our method can be used as a quick and noninvasive tool to measure the strain and hence, the stability, of a commercial foam; it is worth to check the above claim for simple foamy material with well controlled composition, specially made in a laboratory. Further, experiments on known surfactants will also indicate if the observed behavior of the wet foam originates from the characteristics of the surfactant itself or from its foamy structure.

VI. ACKNOWLEDGEMENTS

The authors thank A.K. Sood, IISc, Bangalore; A.K. Sharma, IIT, Kanpur; R. Bandyopadhyay, RRI, Bangalore, for their valuable comments.They are also indebted to T. Pathak, IIT Kharagpur, for his comments on the synthesis of surfactants.

---

[1] Weaire, D.; Hutzler, S. *The Physics of Foams*; Oxford University Press: Oxford, 1999, 215-217.

[2] Weaire, D.; Fortes, M.A. *Adv. in Phys.* **1994**, *43*(6), 685-738.

[3] In ref. [1] see pp. 75-87.

[4] Bolton, F.; Weaire, D. *Phys. Rev. Lett.* **1990**, *65*(27), 3449-3451.

[5] Feng, S.; M.F. Thorpe, M.F.; Garboczi, E. *Phys. Rev. B*, **1985**, *31*, 276-280.

[6] Hutzler, S.; Weaire, D.; Bolton, F. *Phil. Mag. B*, **1995**, *71*(3), 277-289.

[7] Princen, H.M.; Kiss, A.D. *J. Colloid Interface Sci.* **1986**, *112*(2), 427-437.

[8] Durian, D.J. *Phys. Rev. lett.* **1995**, *75*(26), 4780-4783.

[9] Durian, D.J. *Phys. Rev. E* **1997**, *55*(2), 1739-1751.

[10] Nickolov, Zn.S.; Earnshaw, J.C.; Mallamace, F.; N. Micali, N.; Vasi, C. *Phys. Rev. E*, **1995**, *52*(5), 5241-5249.

[11] Davies, R.J.; M. Burghammer, M.; Riekel, C. *Macromolecules*, **2006**, *39*, 4834-4840.

[12] Ward, I and Young, R. J. *Polymer*, **2001**, *42*, 7857-7863.

[13] Heussinger, C.; Frey, E. *Phys. Rev. Lett.* **2006**, *96*, 017802-1-4.

[14] Gautev, N.; Nikolov, Zh.S. *Phys. Rev. E* **1996**, *54*(2), 1725-1733.

[15] Barik, T.K.; Ojha, A.K.; Roy, A. *J. Raman Spectroscopy*, **2008** (in press).

[16] Singha, A.; Dhar, P.; Roy, A. *Am. J. Phys.* **2005**, *73*(3), 224-233.

[17] Coughlin, M.F.; Ingenito, E.P.; Stamenovic, D. *J. of Colloid and Interface Science*, **1996**, *181*, 661-666.

[18] Snyder, R.G. *J. Chem. Phys.* **1967**, *47*(4), 1316-1359.

[19] Cerdeira, F.; Buchenauer, C.J.; Pollak, F.H.; Cardona, M. *Phys. Rev. B*, **1972**, *5*(2), 580-593.

[20] Aubert, J.H.; Kraynik, A.M.; Rand, P.B. *Sci. Am.* **1986**, *254*, 74-82.

[21] Durian, D.J.; Weitz, D.A.; Pine, D.J. *Science* **1991**, *252*, 686-688.

[22] In ref. [1] see p. 91.

[23] Stine, K.J.; Rauseo, S.A.; Moore, B.J. *Phys. Rev. A* **1990**, *41*(12), 6884-6893.

[24] Frieberg, A.C and Langlois, B.C, *Langmuir* **1994**, *10*, 2939.

[25] Tiddy, G.J.T, *Phys. Rep.*, **1980**, *57C*, 1.

[26] Infrared and Raman characteristic group frequencies, Tables and Charts. Third edition. by G. Scorates, John Wiley and Sons. Ltd. pp. 52-53.

[27] N. Yellin and I.W. Levin, BioChim. Biophys. Acta, **489**, 177 (1977).

[28] S.B. Dierker, C.A. Murray, J.D. Legrange and N.E. Scholotter, Chem. Phy. Lett. **137**, 453 (1987).